A V2V Channel Simulator for Velocity Variations in Non-isotropic Scattering Scenarios

Naeem Ahmed, Boyu Hua, Qiuming Zhu(✉), and Mao Kai

College of Electronic and Information Engineering, Nanjing University of Aeronautics and Astronautics, Nanjing 211106, China
{jubayar123,byhua,zhuqiuming,maokai}@nuaa.edu.cn

Abstract. Based on the consideration of variations in the velocity of both the mobile transmitter (MT) and the mobile receiver (MR), the method of vehicle-to-vehicle (V2V) channel simulation is mentioned in this letter. This method is able to simulate non-stationary fading channels under non-isotropic scattering scenarios. In which, the time variant parameters, i.e., complex channel coefficient, path power, and path delay are analyzed and derived. The proposed method can also be used for the real V2V communications by considering the effect of velocity variations on the channels. Besides, the analytical mathematical properties, i.e., probability density function (PDF), auto-correlation function (ACF), Doppler power spectral density (DPSD) are studied and executed under the Von Mises (VM) distribution. Simulation results show a well understanding between the analytical and emulated results, which ensures the efficiency of both the suggested method and derivations.

Keywords: Channel simulator · Non-isotropic scattering scenario · Statistical properties · V2V channel · Velocity variation

1 Introduction

V2V propagation channels have a great importance on the purpose and execution of novel communication protocols for vehicular ad hoc networks (VANETs) [1]. With consideration of a general design for non-stationary V2V channels with moving scatterers and terminal velocity variations [2] i.e., the mobile-to-mobile non-stationary (M2M) channel model introduced with dynamic velocities and trajectories [3]. Under multiple conditions, the channel model plays an essential role in designing, validation and optimization of communication system output [4]. The V2V communication is one of the most valuable communication systems, which can upgrade the security of life and resources by gathering and transferring information under sophisticated transportations [5]. In the meantime, fifth generation (5G) systems in [6] considered multiple-input multiple-output (MIMO) and V2V technologies for improving efficiency and develop the communication performance.

M. Guan and Z. Na (Eds.): MLICOM 2020, LNICST 342, pp. 447–458, 2021.
https://doi.org/10.1007/978-3-030-66785-6_49

The geometry-based stochastic model (GBSM) is a mainstream kind of modeling V2V channel in recent years due to its moderate accuracy and complexity. The channel is always changing constantly in the real world due to the moving objects and multiple-bounce scattering [3,7]. So, the assumption of the channel statistics does not change within a specific time and frequency [8]. The assumption of wide-sense stationary (WSS) modeling valid is only for very short time intervals, therefore in [9] a non-WSS V2V regular-shaped GBSM (RS-GBSM) is proposed. However, a large number of measured results show that the characteristics of V2V channel change with the scattering environment, i.e. the non-stationary feature of the V2V channel [10]. Besides, some existing models can be assorted as the movements in [11,12], imperfect receiver places in [13,14], and inadequate scatterers in [15,16] which investigated in channel modeling and statistical properties. Non-stationary V2V channel model is introduced in [17] which is much more accurate with real world GBSMs and also in [18] the model depicted the street scatterers, and supported for MIMO and wideband system. The non-stationary V2V channels allowed different velocities for both stable and moving scatterers. For both the LOS and NLOS cases, moving scatterers have an important contribution in the wideband V2V channels. In addition, increase and decrease tap powers, Doppler power spectral desity (PSD) and root-mean-square (rms) Doppler spread, reduce the rms delay spread in both LOS and NLOS scenarios. It can also increase the capacity for the LOS scenario, but for the NLOS scenario it has little impact [19]. In order to accord with non-isotropic scattering conditions, the sum-of-cisoids (SOC) simulation method was introduced in [20], which is better fitting with the measurements. By comparing the generalized method of equal areas (GMEA) with the Lp-norm method (LPNM) in [20,21] for designing SOC simulators has less time complexity and makes model parameters simpler while applying GMEA. The model in [22] V2V GBSM takes into account the variation in velocity of terminals along with moving scatterers, the measurement of real-time channel parameters and movements at different traffic conditions. The complex channel coefficient which is much more complicated comes to in consideration in this paper. The corresponding statistical properties i.e., PDF, ACF, and DPSD are also studied and executed under VM distribution scattering scenarios.

The remainder of the paper is structured according to this. Section 2 describes the reference model. Section 3 gives the proposed simulator and parameter computation method. The statistical properties of proposed method are executed in Sect. 4. The simulation and analyzed results are conducted in Sect. 5. At last, conclusions are drawn in Sect. 6.

2 Reference Model

Under a standard V2V communication scenario, the transmitter and receiver are moving with time-variant velocities, which can be denoted as v^T and v^R, accordingly. There are several propagation paths in the V2V communication system, and each path includes several sub-paths. The velocities of T and R are

in an initial distance, in which the angle between arrival signal with the direction of movements can be at the linear form of velocity variations [23].

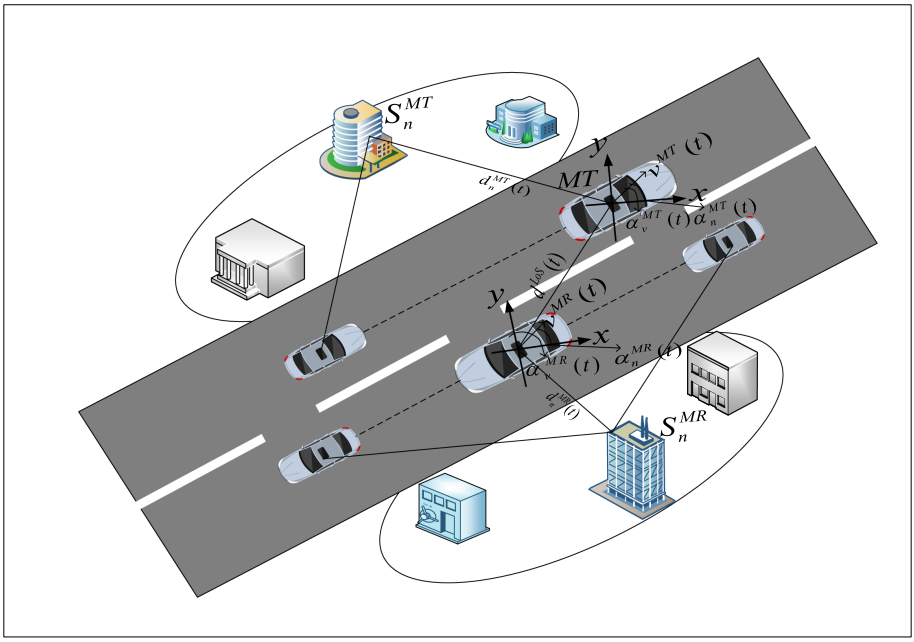

Fig. 1. A communication scenario of V2V channel model with velocity variations.

The time-variant channel impulse response (CIR) between the transmission and the receiver can be represented under non-stationary scattering scenarios as [24,25]

$$h(t,\tau) = \sum_{n=1}^{N(t)} \sqrt{P_n(t)} h_n(t) \delta(\tau - \tau_n(t)) \tag{1}$$

where $N(t)$ is the number of propagation paths distinguished by path delay $\tau n(t)$, path power $P_n(t)$ and channel coefficient $h_n(t)$. In (1) path delay $\tau_n(t)$ can be described as $\tau_n^T(t) + \tau_n^R(t) + \tilde{\tau}_n(t)$, where $\tau_n^T(t)$ and $\tau_n^R(t)$ explain the time delays of both the transmitter and receiver accordingly. And $\tilde{\tau}_n(t)$ describes the virtual link's equivalent pause. Additionally, it is also possible to model $h_n(t)$ by summing infinite sub-paths [24,26],

$$h_n(t) = \lim_{N\to\infty} \frac{1}{\sqrt{N}} \sum_{N=1}^{N} \exp\left\{ j(2\pi \int_0^t f_n(t)dt + \theta_n) \right\} \tag{2}$$

where N specifies the number of sub-paths, $f_n(t)$ is the time-variant Doppler frequency and the phase θ_n is periodic over $[\pi, -\pi)$ and can be represented as an independent, evenly distributed random variable over $[\pi, -\pi)$.

The channel impulse response (CIR) between T and R can be expressed as (1) under the general scattering environment, where N is the number of multi-paths and sub-paths in each path, in (1) $h_n(t)$ represents the complex channel coefficient and can be expressed as

$$h_n(t) = \exp\left\{j(2\pi \int_0^t f_n(t)dt + \theta_n)\right\} \tag{3}$$

where $f_n(t)$ is the time-variant Doppler frequency and the initial phase θ_n is periodical over $[\pi, -\pi)$. And f_n is the discrete Doppler frequencies and can be calculated by

$$f_n(t) = \frac{v^T(t)\cos\alpha_n^T(t) + v^R(t)\cos\alpha_n^R(t)}{\lambda} \tag{4}$$

where v denotes the amplitude of velocity, λ is the wave number, and α_n is the angle between arrival signal with the direction of movement. It should be mentioned that parameters $\{\theta_n, f_n\}$ are constant during each simulation trial under stationary scattering environments. In this paper $h_n(t)$ is modeled as an infinite sub-path superposition. Our proposed model can be acquired by replacing the current Doppler frequency model into (2). Note that our model is only designed for the complex channel coefficient $h_n(t)$ which is very complex to simulate rather than the power path $P_n(t)$ and path delay $\tau_n(t)$.

3 Proposed Simulator and Parameter Computation Methods

3.1 Proposed Simulation Method

The proposed method can be denoted as

$$\tilde{h}(t) = \frac{\sigma_\mu}{\sqrt{N}} \sum_{n=1}^{N} \exp\left\{j\left(2\pi\tilde{f}_n t + \theta_n\right)\right\} \tag{5}$$

where N is the number of cissoids, θ_n is the initial phase of each path and can be developed by distinct random variables evenly distributed over $[-\pi, \pi)$. Doppler frequencies will be time-variant for the non-stationary situation due to changes of angles or velocities over time which can be modified as

$$\tilde{f}_n(t) = \frac{1}{\lambda}\left(v^T(t)\cos\alpha_n^T(t) + v^R(t)\cos\alpha_n^R(t)\right). \tag{6}$$

Most of existing non-stationary simulators or emulators use formula of $2\pi\tilde{f}_n(t)t$ directly to update the denoted model. In this case, the time-variant Doppler frequencies of generated fading channels would be

$$\int_0^t \tilde{f}_n(t)dt = \int_0^t \left(v^T(t)\cos\alpha_n^T(t) + v^R(t)\cos\alpha_n^R(t)\right)dt. \tag{7}$$

To overcome this shortcoming, submitting (7) into (5) which can be denoted as

$$\hat{\mu}(t) = \frac{\sigma_\mu}{\sqrt{N}} \sum_{n=1}^{N} \exp\left\{ j\left(\frac{2\pi}{\lambda} \int_0^t \left(\begin{pmatrix} v^T(t)\cos\alpha_n^T(t) + \\ v^R(t)\cos\alpha_n^R(t) \end{pmatrix} dt \right) + \theta_n \right) \right\}. \tag{8}$$

3.2 Computation of Time-Variant Doppler Frequencies

For the case of stationary scattering environments, i.e., isotropic scattering scenario, the angles follow a fixed distribution and can be approximated as independent with time instants or the locations of transceiver. Thus, the time-variant Doppler frequencies only depend on the amplitude of velocity. For a short time period, the speed can be approximated by a linear model [27],

$$\begin{aligned} v^T(t) &= v_0^T + a_0^T t \\ \alpha^T(t) &= \alpha_{n,0}^T + b_0^T t \end{aligned} \tag{9}$$

$$\begin{aligned} v^R(t) &= v_0^R + a_0^R t \\ \alpha^R(t) &= \alpha_{n,0}^R + b_0^R t \end{aligned} \tag{10}$$

where v_0, a_0 are constants describing the initial velocity and the rate-of-change of velocity. Submitting (9), (10) and (6) into (8), our simulation model can be simplified as

$$\begin{aligned} \hat{h}(t) =& \frac{\sigma_\mu}{\sqrt{N}} \sum_{n=1}^{N} e^{j\left\{ \frac{2\pi}{\lambda} \int_0^t \begin{pmatrix} (v_0^T + a_0^T t)\cos(\alpha_0^T + b_0^T t) \\ +(v_0^R + a_0^R t)\cos(\alpha_0^R + b_0^R t) \end{pmatrix} dt + \theta_n \right\}} \\ =& \frac{\sigma_\mu}{\sqrt{N}} \sum_{n=1}^{N} e^{j\left\{ \frac{2\pi}{\lambda} \begin{pmatrix} (v_0^T \cos\alpha_{n,0}^T t + (a_0^T \alpha_{n,0}^T + b_0^T v_0^T)\frac{t^2}{2} \\ +a_0^T b_0^T \frac{t^3}{3}) + (v_0^R \cos\alpha_{n,0}^R t + \\ (a_0^R \alpha_{n,0}^R + b_0^R v_0^R)\frac{t^2}{2} + a_0^R b_0^R \frac{t^3}{3}) \end{pmatrix} + \theta_n \right\}}. \end{aligned} \tag{11}$$

It is noticed that this simplified model has been studied in [28–30]. In this case each path behaves like a chirp signal or a linear frequency modulation (LFM) signal, thus it is named as the sum-of-chirps model or the sum-of-LFM method in [28–30].

4 Stochastic Properties for Proposed Methods

4.1 Time-Variant PDF

For deriving the PDF of the proposed model here it can be described as

$$\hat{\mu}_\xi(t, z) = (2\pi)^2 z \int_0^\infty \left\{ \begin{array}{l} j_0(2\pi\sqrt{\frac{\sigma_\mu(t)K(t)}{K(t)+1}}x)\cdot \\ \prod_{m=1}^{M} j_0(2\pi\sqrt{\frac{\sigma_\mu(t)}{N(K(t)+1)}}x)\cdot \\ j_0(2\pi z x)\cdot x \end{array} \right\} dx. \tag{12}$$

In (12) it shows that $\hat{h}_{\xi}(t,z)$ can entirely described by the variables of $N, \sigma_{\mu}(t)$ and $K(t)$, while the frequency variables have no impact. Thus, at every time period $\sigma_{\mu}(t)$ and $K(t)$ are stable. The PDF simulation model to obtain the output channels to the same components and quadrature components.

4.2 Time-Variant ACF

The ACF for non-isotropic scattering scenarios is a time-variant and corresponds both functions of time lag τ and time t. The time-variant ACF could be specified as

$$\begin{aligned} r_{hh}(\tau) &= r_{mm}(\tau) + r_{\mu\mu}(\tau) \\ &= E\{m^{*}(t)\, m(t+\tau)\} + E\{\mu^{*}(t)\, \mu(t+\tau)\} \end{aligned} \tag{13}$$

where $r_{mm}(\tau)$ and $r_{\mu\mu}(\tau)$ denotes the path components respectively. Here $r_{mm}(\tau)$ can be approximately calculated by

$$r_{\tilde{m}\tilde{m}}(t,\tau) = \exp\left\{ j2\pi \int_{t}^{t+\tau} \tilde{f}_{n}(\tau) d\tau \right\} =$$

$$\exp\left\{ j\frac{2\pi\tau}{\lambda} \left[\left\{ \begin{pmatrix} v_0^T \cos\alpha_{n,0}^T(\tau) + \\ (a_0^T \alpha_{n,0}^T + v_0^T b_0^T) \\ (t\tau + \frac{\tau^2}{2}) + a_0^T b_0^T \\ (t^2\tau + t\tau^2 + \frac{\tau^3}{3}) \end{pmatrix} + \left\{ \begin{pmatrix} v_0^R \cos\alpha_{n,0}^R(\tau) + \\ (a_0^R \alpha_{n,0}^R + v_0^R b_0^R) \\ (t\tau + \frac{\tau^2}{2}) + a_0^R b_0^R \\ (t^2\tau + t\tau^2 + \frac{\tau^3}{3}) \end{pmatrix} \right\} \right] \right\}. \tag{14}$$

The calculation of (14) shows the ACF changes over time-delay. The time-variant ACF with the VM distribution can be specified as

$$\tilde{r}_{\tilde{\mu}\tilde{\mu}}(\tau) = \sum_{s}^{\{1,2\}} \prod_{i}^{\{T,R\}} E\left\{ \left(\tilde{\mu}_s^i(t)\right)^{*} \tilde{\mu}_s^i(t+\tau) \right\}. \tag{15}$$

Finally, the theoretical ACF in (13) of the proposed model can be obtained by substituting (13) and (14) into (15).

4.3 Time-Variant DPSD

The time-variant DPSD could be represented as

$$\tilde{S}_{\tilde{h}\tilde{h}}(f) = \int_{-\infty}^{\infty} \tilde{r}_{\tilde{h}\tilde{h}}(t,\tau) \exp\{-j2\pi f\tau\} d\tau. \tag{16}$$

For Doppler frequencies linear variation, we know

$$\mu(t) = \frac{\sigma}{\sqrt{N}} \sum_{n=1}^{N} \exp\left\{ j\left[2\pi\left(f_n t + \frac{k_n}{2} t^2 \right) + \theta_n \right] \right\}. \tag{17}$$

By the support of the Wigner-ville method the DPSD can be written as,

$$W_\mu(f,t) = \frac{\sigma^2}{N}\sum_{n=1}^{N}\delta(f - f_n - k_n t) + 4\sum_{n=1}^{N-1}\sum_{\substack{m=2\\ m>n}}^{N}\frac{\sigma^2}{\sqrt{\beta_{nm}}}\cos\left(\frac{\pi}{4} + \alpha_{nm} - \frac{4\pi\gamma_{nm}^2}{\beta_{nm}}\right) \tag{18}$$

where,

$$f_n = \frac{v^T\cos\alpha_n^T + v^R\cos\alpha_n^R}{\lambda} \tag{19a}$$

$$\alpha_{nm} = \theta_n - \theta_m + 2\pi\left(\frac{v^T\cos\alpha_n^T + v^R\cos\alpha_n^R}{\lambda}\right)t + \pi\left(k_n - k_m\right)t^2 \tag{19b}$$

$$\beta_{nm} = k_n - k_m \tag{19c}$$

$$\gamma_{nm} = f - \left(\frac{v^T\cos\alpha_n^T + v^R\cos\alpha_n^R}{2\lambda} + \frac{k_n - k_m}{2}t\right). \tag{19d}$$

The initial phase is random and evenly spaced over $[0, 2\pi)$ hence the equation (18) could be withdrawn by building over the phases. Thus, the DPSD could be written as

$$S_\mu(f,t) = W_\mu(f,t)|_{\bar{\theta}_n} = \frac{\sigma^2}{N}\sum_{n=1}^{N}\delta\left(f - (\frac{v^T\cos\alpha_n^T + v^R\cos\alpha_n^R}{\lambda}) - k_n t\right). \tag{20}$$

5 Simulated and Analyzed Results

The proposed model validated under typical V2V scenarios which is verified by computing both theoretical and simulated results. In this proposed simulation method different trajectories are considered for the different variations of MT and MR, i.e., the similar directions, the inverse directions. By considering those different scenarios the VM distribution with $\kappa = 1$ and the carrier frequency is 2.40 GHz. The movements of scatterers are evenly distributed around terminals and all the parameters also random with various scenarios. As for validating the simulation output along with the theoretical output we considered PDF, ACF and DPSDs at several time instants.

According to (12) in this method the output of PDFs at three different time periods where t = 0 s, 1 s and 2 s is differentiated with the analytical results in Fig. 2. Similarly, for comparing the analytical and emulated ACFs at three different time periods where t = 0 s, 1 s and 2 s is derived and established in

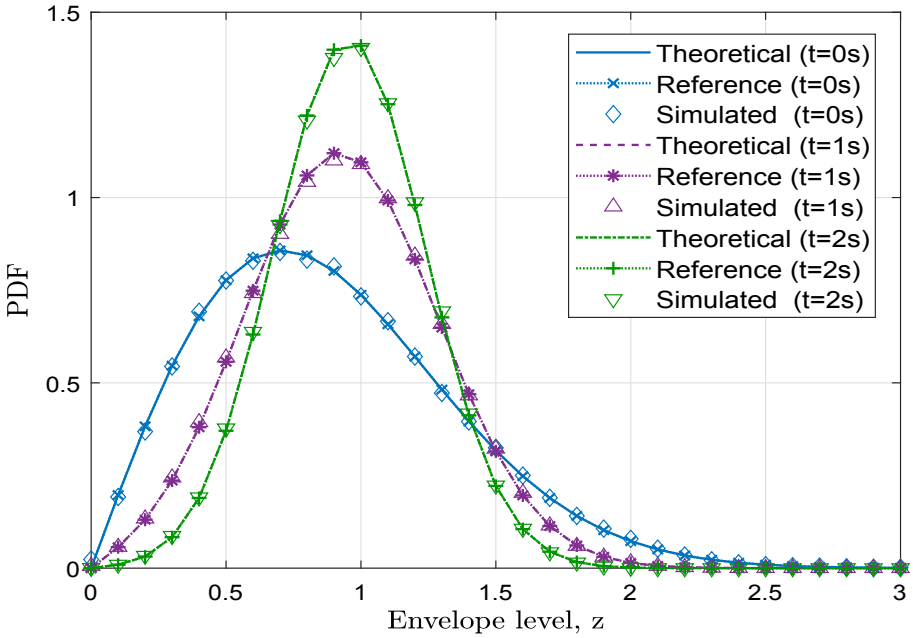

Fig. 2. Theoretical and simulated PDFs at different time instants.

Fig. 3. The simulation values generated by the improved method proposed in this paper are consistent with the analytical values of the reference model, and as the simulation time increases, both the PDFs and ACFs of the channel changes from Rayleigh distribution (t = 0 s) to Rice distribution (t = 1 s, 2 s). It should be noted that the larger the number of times the simulation, the closer the value of the simulation will be to the analytical value and the higher the accuracy of the simulation. As for the different time periods the simulated results of PDFs and ACFs showed a well matched results with the corresponding analytical results, which verifies simulated results with the analytical ones. Figures 2 and 3 shows a good agreement at different time instants.

Besides, the analytical DPSDs established by (16) are given in Figs. 4 and 5 which apparently shows the time divergence of the LOS components along with time path by the effect of velocity variations under different scenarios. Scatterers movements are considered to be evenly distributed across terminals. The T and R are shifting in two different scenarios along with different velocity patterns. Thus, the Doppler frequencies are computed and differentiate in Figs. 4 and 5 which shows that, the maximum Doppler shift in Scenario I and Scenario II are slightly changed from each other which also specifies the movements of scatterer. Those figures clearly show that the emulated Doppler frequencies of the designed method suited well with the analytical ones. As for the Doppler frequencies shifting overtime which can clearly be observed, means the velocity parameters v^T, v^R and also the acceleration parameters a^T, a^R are affecting the Doppler shifts

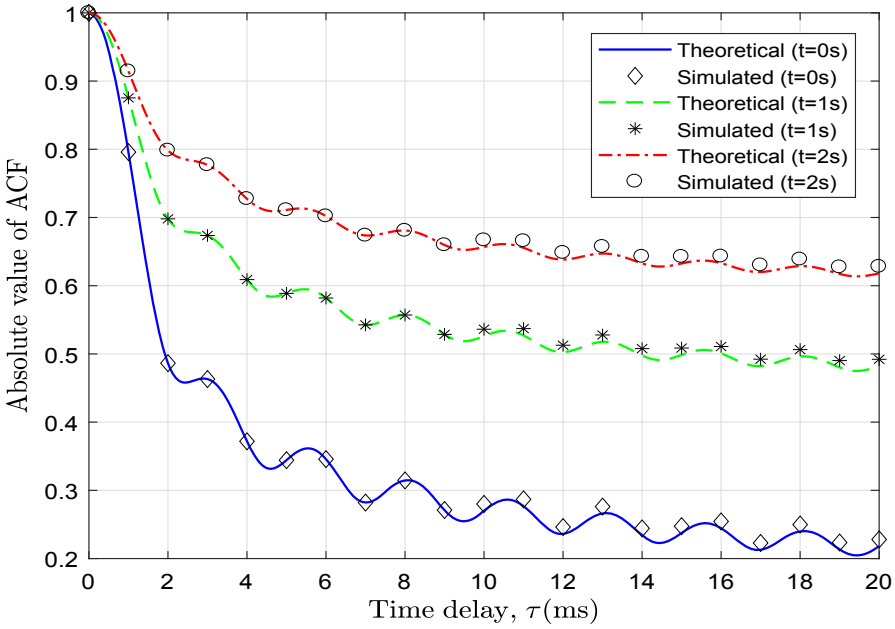

Fig. 3. Theoretical and simulated ACFs at different time instants.

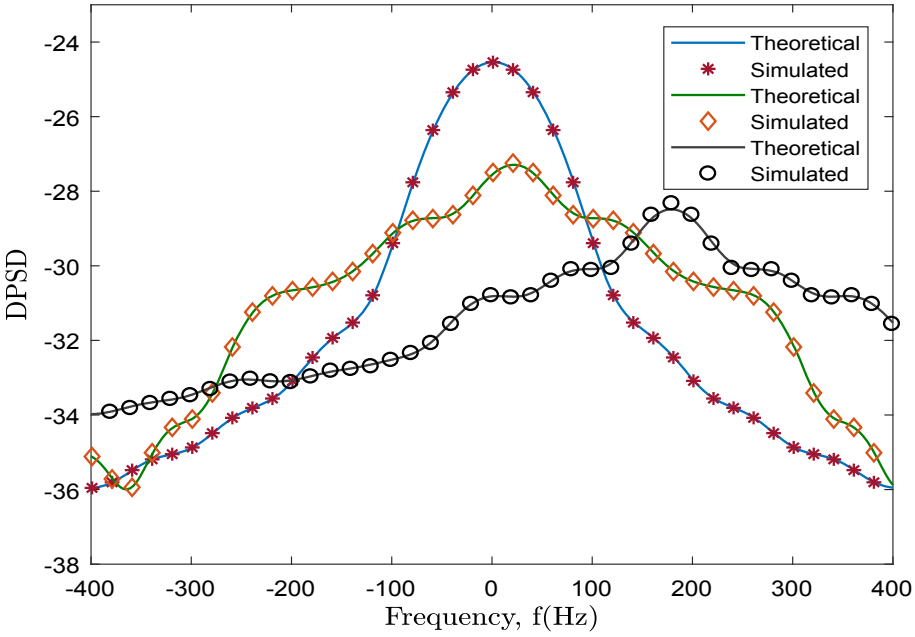

Fig. 4. DPSDs at different time instants under scenario I.

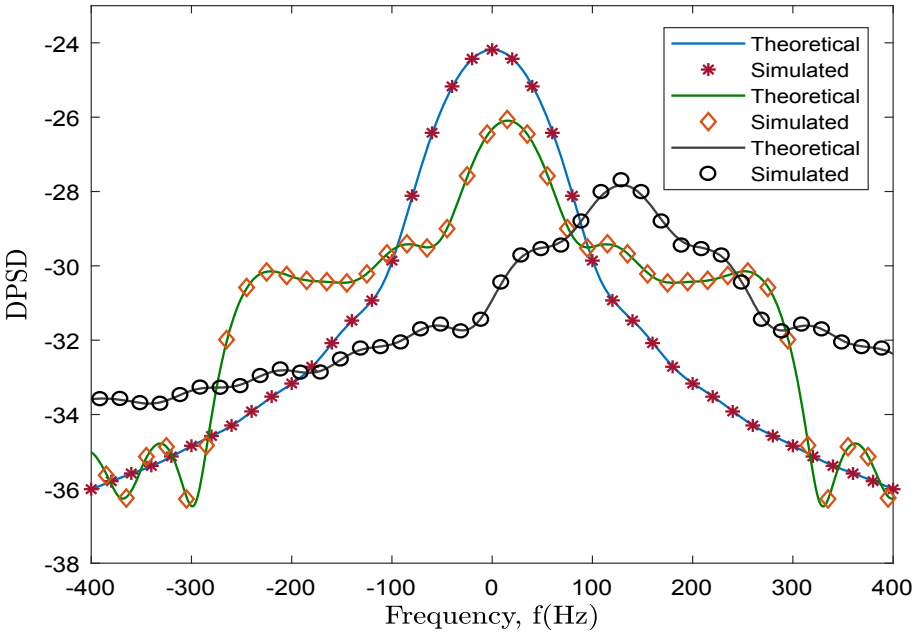

Fig. 5. DPSDs at different time instants under scenario II.

along with time, which proves the perfect understanding between the analytical and emulated results. Figures 4 and 5 shows that, the DPSD of analytical and emulated results for the first and second scenario of velocity variations with moving scatterers respectively, which is the results of the non-isotropic scattering scenarios. Finally, the well understanding of the analytical and simulated results in Figs. 4 and 5 confirms the accuracy, as well as the proposed model.

6 Conclusions

This letter mentioned a V2V channel simulator for velocity variations in non-isotropic scattering scenarios, which allows velocity variations of both MT and MR. By adjusting the channel parameters, the effort of the velocity variations on the channel characteristics specifically exposed. The parameter computation methods of time-variant simulations are given. Based on this simulation method, the analyzed results for different time instants of the PDFs, ACFs and DPSDs under VM distribution scattering scenarios are derived. Simulated results also show that the proposed model provides very close approximations to the analytical results.

Acknowledgments. This work was supported in part by the National Key Scientific Instrument and Equipment Development Project under Grant No. 61827801, in part by Aeronautical Science Foundation of China, No. 201901052001, and in part by the Fundamental Research Funds for the Central Universities, No. NS2020026.

References

1. Abbas, T., Sjöberg, K., Karedal, J., Tufvesson, F.: A measurement based shadow fading model for vehicle-to-vehicle network simulations. Int. J. Antennas Propag. 2015, Art. ID 190607, May 2015
2. Zhu, Q., Li, W., Wang, C.-X., Xu, D., Bian, J., et al.: Temporal correlations for a nonstationary vehicle-to-vehicle channel model allowing velocity variations. IEEE Commun. Lett. **23**(7), 1280–1284 (2019)
3. He, R., Ai, B., Stüber, G.L., Zhong, Z.: Mobility model-based nonstationary mobile-to-mobile channel modeling. IEEE Trans. Wireless Commun. **17**(7), 4388–4400 (2018)
4. Fei, D., He, R., Ai, B., Zhang, B., Guan, K., et al.: Massive MIMO channel measurements and analysis at 3.33 GHz. In: 10th International Conference on Communcation and Network in China (ChinaCom), pp. 194–198, August 2015
5. Wang, C.-X., Cheng, X., Laurenson, D.I.: Vehicle-to-vehicle channel modeling and measurements: recent advances and future challenges. IEEE Commun. Mag. **47**(11), 96–103 (2009)
6. Wang, C.-X., Bian, J., Sun, J., Zhang, W., Zhang, M.: A survey of 5G channel measurements and models. IEEE Commun. Surv. Tuts. **20**(4), 3142–3168 (2018)
7. Ghazal, A., Wang, C.-X., Ai, B., Yuan, D., Haas, H.: A nonstationary wideband MIMO channel model for high-mobility intelligent transportation systems. IEEE Trans. Intel. Trans. Sys. **16**(2), 885–897 (2015)
8. Herdin, M.: Non-stationary indoor MIMO radio channels, Ph.D. dissertation, Technische Universitat Wien, August 2004
9. Yuan, Y., Wang, C.-X., He, Y., Alwakeel, M.M., Aggoune, E.M.: 3D wideband non-stationary geometry-based stochastic models for nonisotropic MIMO vehicle-to-vehicle channels. IEEE Trans. Wireless Commun. **14**(12), 6883–6895 (2015)
10. Dahech, W., Pätzold, M., Gutiérrez, C.A., Youssef, N.: A non-stationary mobile-to-mobile channel model allowing for velocity and trajectory variations of the mobile stations. IEEE Trans. Wireless Commun. **16**(3), 1987–2000 (2017)
11. Guan, K., Ai, B., Nicolas, M.L., Geise, R., Moller, A., Zhong, Z., et al.: On the influence of scattering from traffic signs in vehicle-to-X communications. IEEE Trans. Veh. Technol. **65**(8), 5835–5849 (2016)
12. Cheng, X., Wang, C.-X., Ai, B., Aggoune, H.: Envelope level crossing rate and average fade duration of nonisotropic vehicle-to-vehicle ricean fading channels. IEEE Trans. Intell. Transp. Syst. **15**(1), 62–72 (2014)
13. Zhu, Q., Xue, C., Chen, X., Yang, Y.: A new MIMO channel model incorporating antenna effects. Prog. Electromagn. Res. M **50**, 129–140 (2016)
14. Zajic, A.G., Stuber, G.L.: Space-time correlated mobile-to mobile channels: modelling and simulation. IEEE Trans. Veh. Technol. **57**(2), 715–726 (2008)
15. Fan, W., de Lisbona, X.C.B., Sun, F., Nielsen, J.Ø., Knudsen, M.B., Pedersen, G.F.: Emulating spatial characteristics of MIMO channels for OTA testing. IEEE Trans. Antenna Propag. **61**(8), 4306–4314 (2013)
16. Zhang, J., Zhang, X., Yu, Y., Xu, R., Zheng, Q., et al.: 3D MIMO: how much does it meet our expectations observed from channel measurements. IEEE J. Sel. Areas Commun. **35**(8), 1887–1903 (2017)
17. Zhu, Q., Yang, Y., Chen, X., Tan, Y., Fu, Y., Wang, C.-X., et al.: A novel 3D non-stationary vehicle-to-vehicle channel model and its spatial-temporal correlation properties. IEEE Access **6**, 43633–43643 (2018)

18. Zhao, X., Liang, X., Li, S., Ai, B.: Two-cylinder and multi-ring GBSSM for realizing and modeling of vehicle-to-vehicle wideband MIMO channels. IEEE Trans. Intel. Trans. Sys. **17**(10), 2787–2799 (2016)
19. Liang, X., Zhao, X., Li, Y., Li, S., Wang, Q.: A non-stationary geometry-based street scattering model for vehicle-to-vehicle wideband MIMO channels. Wireless Pers. Commun. **90**(1), 325–338 (2016)
20. Gutiérrez, C.A., Pätzold, M.: The generalized method of equal areas for the design of sum-of-cisoids simulators for mobile Rayleigh fading channels with arbitrary Doppler spectra. Wirel. Commun. Mob. Comp. **13**(10), 951–966 (2013)
21. Gutiérrez, C.A.: Channel Simulation Models for Mobile Broadband Communication Systems. University of Agder, Kristiansand (2009)
22. Li, W., Chen, X., Zhu, Q., Zhong, W., Xu, D., et al.: A novel segment-based model for non-stationary vehicle-to-vehicle channels with velocity variations. IEEE Access **7**, 133442–133451 (2019)
23. Li, J., Jiang, D., Zhang, X.: DOA estimation based on combined unitary ESPRIT for coprime MIMO radar. IEEE Commun. Lett. **21**(1), 96–99 (2017)
24. Zhu, Q., Li, H., Fu, Y., Wang, C.-X., Tan, Y., Chen, X.: A novel 3D non-stationary wireless MIMO channel simulator and hardware emulator. IEEE Trans. on Commun. **66**(9), 3865–3878 (2018)
25. Wu, S., Wang, C.-X., Aggoune, H.M., Alwakeel, M.M., You, X.-H.: A general 3D non-stationary 5G wireless channel model. IEEE Trans. Commun. **66**(7), 3065–3078 (2018)
26. Patzold, M., Gutierrez, C.A.: Definition and analysis of quasi-stationary intervals of mobile radio channels Invited paper. In: Proc, pp. 1–6. IEEE VTC Spring, Porto, Portugal, June 2018
27. Pätzold, M.: Mobile Radio Channels, 2nd edn. Wiley (2012)
28. Pätzold, M., Gutierrez, C.A.: The Wigner distribution of sum-of-cissoids and sum-of-chirps processes for the modelling of stationary and non-stationary mobile channels. In: IEEE 83rd Veh. Tech. Conf. (VTC Spring), pp. 1–5, May 2016
29. Zhu, Q., Liu, X., Yin, X., Chen, X., Xue, C.: A novel simulator of non-stationary random MIMO channels in Rayleigh fading scenarios. Int. J. Antennas and Prop., 1–9 (2016). Art. ID 3492591
30. Jiang, K., Chen, X., Zhu, Q., Chen, L., Xu, D., Chen, B.: A novel simulation model for non-stationary rice fading channels. Wirel. Commun. Mobile Comput. **2018**(1), 1–9 (2018)